

Imaging and Manipulation of Sawteeth and Tearing Modes in TEXTOR

R.J.E. Jaspers¹, G.M.D. Hogeweij¹, H.K. Park², M. de Bock¹, I.G.J. Classen¹, C.W. Domier³, A.J.H. Donné¹, H.R. Koslowski⁴, Y. Liang⁴, N.J. Lopes Cardozo¹, N.C. Luhmann Jr³, A. Merkulov¹, F.C. Schüller¹, S.K. Varshney¹, E. Westerhof¹, O. Zimmermann⁴ and TEXTOR-team⁴

- 1) FOM Institute for Plasma Physics Rijnhuizen*, Association EURATOM-FOM, Nieuwegein, Netherlands
- 2) Princeton Plasma Physics Laboratory, Princeton, New Jersey, U.S.A
- 3) University of California at Davis, Dept. of Applied Science, Davis, California, U.S.A
- 4) Forschungszentrum Jülich, Inst. für Plasmaphysik*, Association EURATOM-FZJ, Jülich, Germany

e-mail contact of main author: r.jaspers@fz-juelich.de

Abstract. The real-time detection and control of instabilities in a thermonuclear plasma presently is and will continue to be one of the exciting challenges in fusion research on the way to a fusion reactor, as will be the understanding of these mechanisms. Through the combination of an innovative 2D imaging technique for temperature fluctuations, a versatile ECRH/ECCD system and a unique possibility to externally induce tearing modes in the plasma, TEXTOR is able to make pioneering contributions in this field. This paper focuses on two different aspects: the sawtooth oscillation and the $n=1$ tearing modes. In both cases the 2D-electron cyclotron emission imaging diagnostic (ECEI) can resolve features not attainable before, allowing a direct comparison with theory and in both occurrences the ECRH system is able to control or suppress these instabilities.

1. Introduction

The manipulation of MHD structures is one of the challenges in fusion research on the way to a full control over the plasma. The suppression of neoclassical tearing modes by electron cyclotron current drive (ECCD) to operate the reactor close to its stability limit and the (de)stabilization of sawteeth in the plasma for impurity control are just two major examples showing the importance of this field.

On TEXTOR a coherent programme is executed around this theme, based on three pillars: an advanced and innovative set of high resolution diagnostics to image the MHD structures in the plasma, a versatile ECRH/ECCD system being capable of effectively acting on the MHD structure and finally a flexible set of perturbation coils to externally induce tearing modes in the plasma.

This paper will concentrate on the detailed understanding of the mechanisms at work in dedicated experiments. By applying the above mentioned tools, deeper insight into the physics of the MHD activity and its control could be obtained: i) by 2 dimensional imaging of the temperature evolution during a sawtooth crash, a direct comparison with simulation based on theoretical models was possible; ii) the control of the sawtooth period by ECCD followed the prediction of a model for the crash based on a critical shear; iii) the excitation of tearing modes is governed by the rotation difference between external field and plasma fluid, and iv) the effect of heating in the suppression of these tearing modes could be isolated from other effects, and was shown to be the dominant term for the experiment under consideration.

* Member of the Trilateral Euregio Cluster (TEC)

2. Experimental tools

Before describing the experimental results it is worthwhile to briefly introduce the main characteristics of the tools used in these studies. Specifically, although TEXTOR is simply a standard, medium sized tokamak with a circular cross-section (major/minor radius $R_0/a=1.75/0.46$ m, and typically $I_p=350$ kA, $B_t=2.25$ T), some of its tools are completely unique, allowing for an exciting research programme.

2.1. Electron Cyclotron Emission- Imaging (ECEI)

The 2D ECE-imaging system [1] consists of a vertically distributed 16 element array of heterodyne receivers, which, combined with wide aperture optics, can image a vertical slice of approximately 16 cm in the plasma. Since each receiver element is treated as a conventional second harmonic X mode ECE radiometer with 8 frequency channels, corresponding to a radial coverage of about 7 cm, the system in total can image an area of 16×7 cm² on an array of 16×8 sampling volumes, centered around the mid-plane, see Fig.1. The radial location can be shifted by either changing the local oscillator frequency (tunable from 85 to 130 GHz) or by varying the magnetic field. The resolution amounts to 2 cm in the vertical direction as limited by the optics and 1 cm radially. The time resolution is up to 500 kHz.

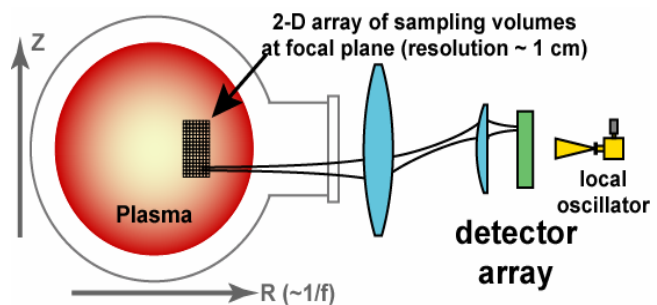


Figure 1: Schematic representation of the ECE-I system, consisting of an 16×8 array of sampling volumes in the plasma.

2.2. Multi pulse TV Thomson Scattering

A novel TV Thomson scattering diagnostic capable of measuring plasma electron temperature (T_e) and density (n_e) profiles at 10 kHz in burst mode is also operational at TEXTOR [2]. This system features a multi-burst 10 kHz ruby laser and an ultra-fast detection system equipped with two CMOS cameras and a cascaded intensifier stage. The detection branch enables to diagnose either the full plasma diameter of 900 mm with 120 spatial elements of 7.5 mm each, or a 160 mm long top edge chord with 98 spatial elements of 1.7 mm each. The recent operation of the system has been performed in a single burst mode consisting of about 20 laser pulses at 5 kHz and with average energy about 15 J giving a sequence of core profiles with statistical errors as low as 7% in T_e and 3% in n_e (at 2.0×10^{19} m⁻³).

2.3. Electron Cyclotron Heating and Current Drive system

A gyrotron operating at 140 GHz is available at TEXTOR, capable of delivering 800 kW during 10 s to the plasma. The flexibility of the system is enhanced by the versatile launcher, which can be tilted both vertically to cover the entire poloidal cross-section as well as toroidally to drive current in either the co- or counter direction [3]. A high degree of localization of the power or current drive can be achieved, which is extremely useful for the experiments on mode suppression. The gyrotron can be operated either continuously (CW) or modulated.

2.4. Dynamic Ergodic Divertor

The Dynamic Ergodic Divertor (DED) on TEXTOR is a set of 16 helical coils on the high field side (HFS), with a helicity aligned with the $q=3$ field lines, with the aim to perturb the magnetic field at the edge of the plasma [4]. The DED can be operated DC and AC up to 10 kHz. It can be used to generate a perturbation field with a dominant 12/4, 6/2, or 3/1 mode structure. When operated in its 3/1 mode it possesses a strong 2/1 side band, which above a certain threshold triggers an $m=2, n=1$ tearing mode. In the experiments reported herein 1 kHz AC currents are used, resulting in a toroidal rotation of 1 kHz for the $m/n = 2/1$ island.

3. Sawteeth

The outstanding phenomenon of the sawtooth instability has important consequences in reactors including helium removal, triggering of neo-classical tearing modes and limiting the maximum attainable core pressure. However, after more than three decades of intensive research, still no conclusive model for the sawtooth crash exists. Recently, using 2D temperature images of the sawtooth crash at TEXTOR unique information could be recorded [5].

3.1. Imaging of the Sawtooth Crash

A typical example of the ECEI images recorded around the inversion radius on TEXTOR are shown in Figure 2. The plasma conditions are quite standard for TEXTOR: plasma current $I_p = 300$ kA, toroidal magnetic field $B_t = 2.0$ T, $n_e(0) = 2.5 \times 10^{19} \text{ m}^{-3}$ and $T_e(0) = 1.5$ keV. For this particular example, the ECEI system is observing at the high field side of the plasma. The general behaviour, however, is the same for observations at the low field side: The hot spot from the core grows and a sharp temperature puncture develops. Initially, this puncture fails to lead to a reconnection, like in frame 4; however, after several attempts (here the second, in frame 9) it succeeds in crossing the inversion radius (curved line in Fig. 2). Then a collective

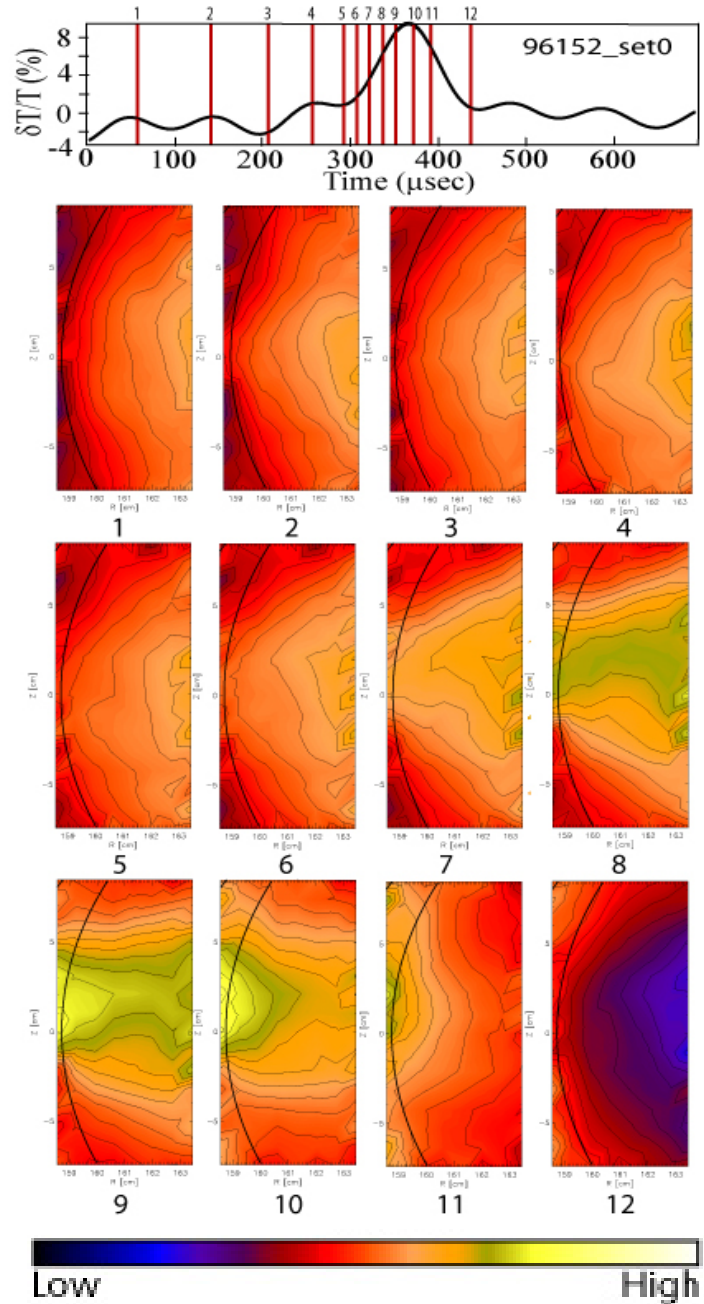


Figure 2: 2-D images from the sawtooth crash at the high field side. A sharp temperature point develops and in the second attempt (frame 9) succeeds to cross the inversion radius through a small opening. The resulting heat flow is highly collective.

outflow of heat takes place after which the symmetry is recovered again (frame 12). The detailed characteristics of the crash pattern are discussed in [6].

Comparing these observations with various theoretical models, only partial agreement is obtained, as discussed in [7]. The first images of the initial reconnection process are similar to those of the pressure driven ballooning mode model, which predicts the development of a temperature bulge as observed here as well. However, the subsequent collective heat outflow is inconsistent with the global stochasticisation of the magnetic field as predicted by simulations based on this model. The quasi-interchange model suggests a convective inflow of colder plasma into the core, contrary to the observations of the sharp temperature puncture, and was therefore falsified. Except for the initial stage (the sharp T_e puncture), the intermediate and final stages of the reconnection process (the collective heat flow), are in agreement with the full reconnection model. To arrive at a conclusive picture, additional measurements are required and planned, with simultaneous observation of high and low field side.

3.2. Manipulation of the Sawtooth Crash

In an attempt to control the sawtooth period, the model by Porcelli was adopted [8]. This model, based on partial reconnection, predicts a triggering of the sawtooth crash when a critical magnetic shear at the $q = 1$ surface is exceeded. With the ECCD system, the effects of localized non-inductive current drive on the sawtooth period could be studied. On the basis of simplified diffusion calculations it was shown that in order to significantly affect the sawtooth period the driven current must satisfy criterion [9]:

$$I_{cd} > 2 \left(\Delta r / r_{q=1} \right)^2 I_{q=1} \quad 1$$

where Δr is the Gaussian width of the driven current profile and $I_{q=1}$ the total current inside the $q=1$ surface, $r_{q=1}$. Co-current deposited inside/outside the $q=1$ surface is expected to speed-up/slow-down the shear evolution at $q=1$ and, consequently, to destabilize/stabilize sawteeth. The reverse is found for counter-current drive.

An experimental study was initiated in order to confirm these model calculations: in a series of discharges the EC power deposition was slowly ramped from close to the center of the plasma to around mid radius by lowering the toroidal magnetic field from 2.5 to 2.1 T during a 3 s period. The plasma current is held constant at 350 kA, and the $q = 1$ radius is near $r/a = 0.3$. The toroidal injection angle (ϕ_{tor}) was varied in order to change the EC driven current

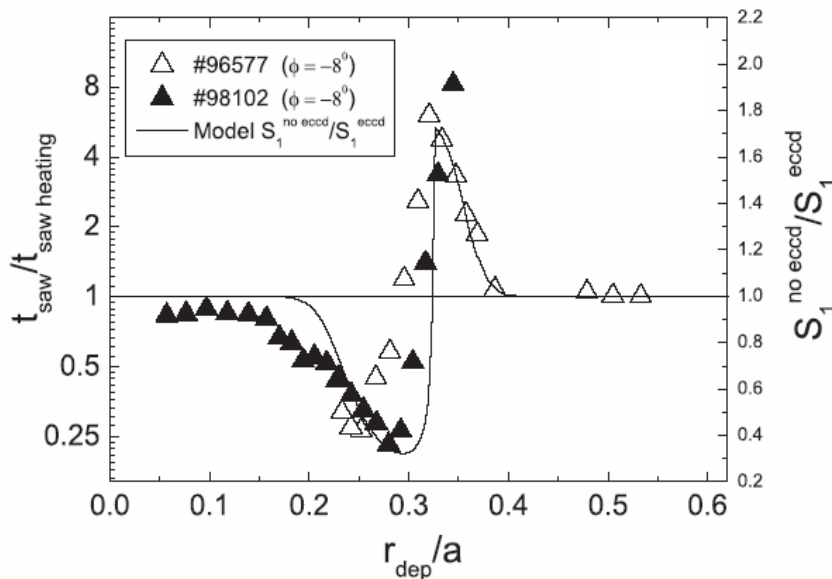


Figure 3: Experimental observations of the sawtooth period in presence of the co-current drive and model calculations of the quantity $S_1^{no\ eccd}/S_1^{eccd}$ for the experimental conditions. The sawtooth period is normalized to the corresponding value in a discharge with pure ECRH as a function of deposition position. The toroidal injection angle of the ECRH launcher is $\phi = -8^\circ$.

from counter-ECCD via almost pure ECRH to co-ECCD. The driven currents as predicted from TORBEAM calculations for the ECCD discharges all satisfied the criterion for sawtooth control (eq. 1). In order to separate the effect of ECCD from the effect of concurrent heating, the ratio of the sawtooth periods of each ECCD discharge and of the ECRH only reference discharge as a function of the EC deposition radius has been studied. Figure 3 shows an example for co-ECCD with $\phi_{tor} = -8^\circ$. For comparison the figure also shows the results of the calculations of the shear evolution model using the driven current and profile widths as predicted for the experimental conditions: plotted is the ratio of the magnetic shear at the $q=1$ surface 20 ms after a sawtooth crash without and with the presence of the additional current drive $s_1^{no\ eccd}/s_1^{eccd}$. This is found to be a reasonable indicator of the regions of shortening and lengthening of the sawtooth period.

In conclusion, these experiments confirm the criterion of Eq. 1, as a reasonable requirement on the non-inductively driven current for effective sawtooth control. In addition, the observed effects of ECCD on the sawtooth period that have been observed support the critical shear model for the sawtooth crash [8].

4. Tearing Mode Studies

Tearing modes can be induced externally at TEXTOR by the DED. This tool provides unique possibilities in the study of tearing mode physics. Here, we treat three of them: the excitation of the mode, the imaging of the mode, and the suppression of the mode. All this can be done in well defined experimental conditions: the perturbation amplitude can be externally governed, the rotation of the perturbation field and the rotation of the plasma can be independently controlled in both directions, by means of the DED and co/counter neutral beam injection, respectively, and finally the gyrotron is able to deposit locally its power inside the island or drive current in the island. If required, this can even be done in phase with the tearing mode.

4.1. Effect of Rotation on Onset of the Tearing Mode

The dependence of the threshold for mode onset (controlled by the DED current) on the plasma rotation has been investigated using the versatile co- and counter neutral beam injectors [10]. The mode threshold has a minimum when the MHD frequency is equal to the frequency of the external perturbation field $f_{DED} = f_{MHD} = f_\phi - f_e^*$, (f_ϕ is the toroidal fluid rotation frequency f_e^* the diamagnetic drift frequency). This has been verified using the dynamic option, i.e. an ac perturbation field, of the DED. The results on the excitation threshold vs the rotation frequency are plotted in Figure 4 for DC and AC⁺ operation. No mode excitation, even at maximum possible coil current, has been obtained when the perturbation field rotated in co-current direction (AC⁻). The difference between the data points for the DC and AC⁺ case is just the 1 kHz rotation of the DED field.

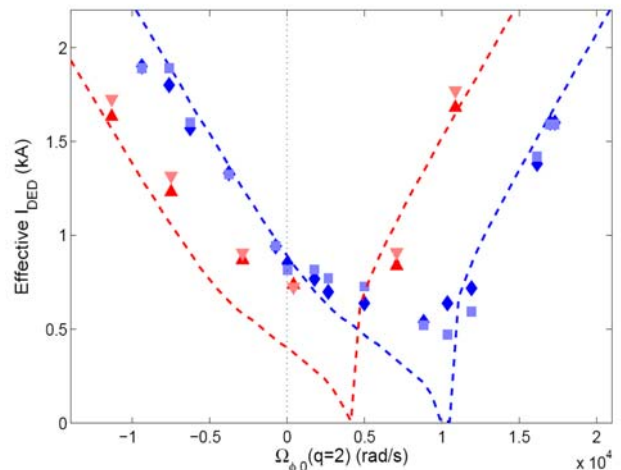


Figure 4: Threshold for mode excitation plotted against the rotation at $q = 2$ before the DED is applied. The density ($1.5 \cdot 10^{19} \text{ m}^{-3}$) and the power input ($\sim \beta$) were kept constant. The data for DC DED operation is given in blue, the data for AC⁺ DED (-1kHz) is given in red. The dotted lines are results of the force balance model.

This experimental finding has been modelled using a linear MHD model taking into account a single mode ($m/n = 2/1$) only. The results are in good agreement with the experiment [11]. The calculated force transfer to the plasma has a maximum when the resonance condition is fulfilled. The same result can be obtained within a simple model balancing the forces acting on the plasma: (i) the momentum input by the heating beams in the centre, (ii) the friction due to charge exchange with neutrals at the edge, (iii) the force arising from edge ergodisation and (vi) the ponderomotive force which tries to synchronize the MHD frequency of the mode with the frequency of the external perturbation field. Force (iii) acts always in co-current direction [12], (ii) is a friction force which always decelerates. The sign of (i) is determined by the net momentum from co- and counter-injection and the sign of (vi) depends on whether the plasma needs to be accelerated or decelerated in order to match the frequencies. The result from this calculation is shown in figure 4 by the dashed lines.

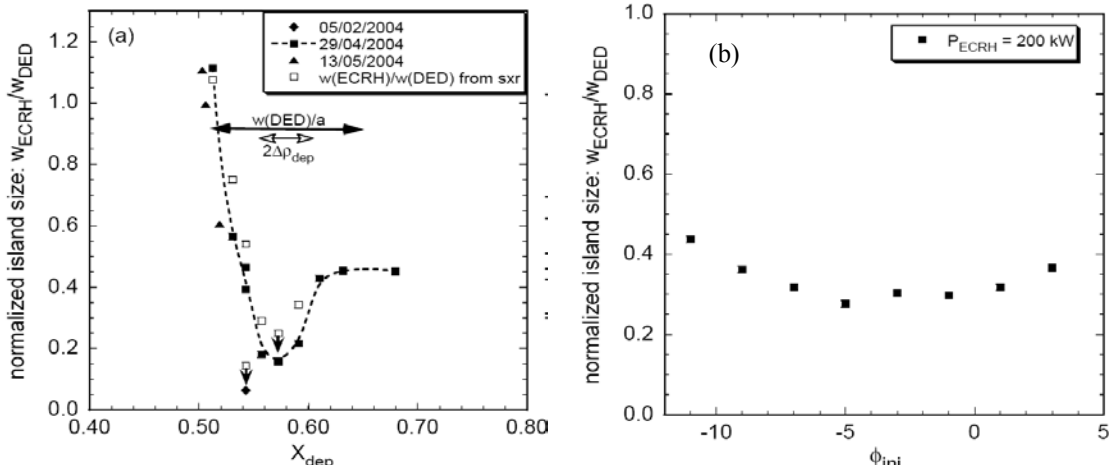


Figure 5: a) Suppression of the 2/1 island due to ECRH, as function of power deposition radius. Depicted is the ratio of the island width, with and without ECRH. Almost complete suppression of the island is obtained if all ECRH power is deposited inside the island.

b) Ratio of island widths versus the toroidal injection angle (measure of the driven current, negative is co-current drive) of the microwave beam. Hardly any change is observed when changing from co- to counter current drive. However, overall an appreciable suppression by a factor of more than 2 is observed, attributed to the heating effect.

4.2. Suppressing of Tearing Modes

Once the mode is excited the flexible ECRH/ECCD tool can be applied to test the scenarios for island suppression. This has contributed to a deeper insight into the relevant processes. Various systematic scans of the mode suppression ratio have been performed, in order to compare (i) ECRH with ECCD, (ii) cw heating with pulsed heating at various duty cycles and (iii) the difference between heating in the X- and O-points of the island. Strongest suppression is found when pulsed ECRH is applied within the O-point of the island [13]. Also, the stabilizing effect hardly changes as the toroidal injection angle and consequently, the driven current is varied. The main results are summarized in Figure 5.

4.3. Imaging of Tearing Mode Evolution

To interpret the physics mechanism at work in suppressing the island, quantitative information on the evolution of the temperature is required. To visualize the ECE-I data in an easily interpretable way, a poloidal reconstruction is used in which the data for one full rotation period are mapped onto a poloidal shell, assuming rigid plasma rotation. Note that this reconstruction only represents the low field side structure of the island. Figure 6 shows the reconstruction of the island during the three main stages of the suppression process [14].

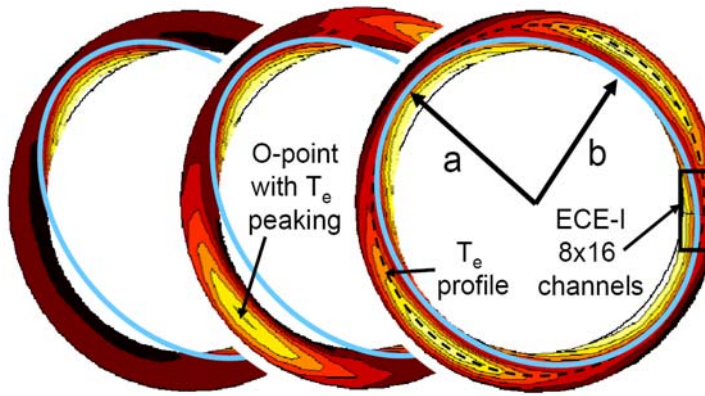


Figure 6: Poloidal reconstructions of the island, showing the time evolution during the suppression process: a) flat island b) heated island c) suppressed island with schematic representation of various island parameters extracted from the poloidal reconstruction, where the island width w is defined as $w=1.5(a-b)$. (The blue line is a isothermal contour of the separatrix. The color coding goes from dark (cold) to light (hot)).

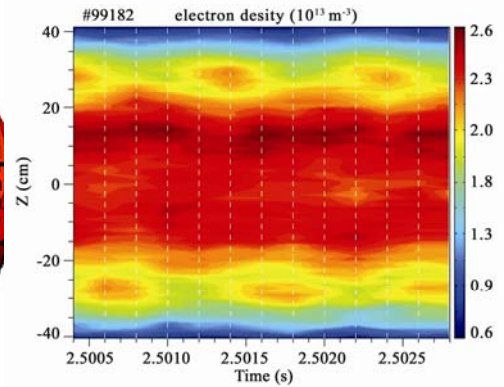


Figure 7: Measurements of density profiles, recorded by the 5 kHz Thomson system. A peaking of the density in the $m=2$ island O-points is observed. The vertical white dashed lines correspond to the measuring times of the Thomson scattering system.

The first stage is the situation in which the island has been generated and has reached a saturated width of about 12 cm, before ECRH was switched on. In this phase, the T_e profile inside the island is still flat. The hot, central plasma, approximately elliptically deformed by the island, is clearly visible. The second reconstruction, shortly (about 10 ms) after switch on of ECRH, shows a peaked T_e profile inside the island. The third stage is the steady state situation long (more than 100 ms) after switch on of ECRH. The island is now suppressed to about half the initial size and the central plasma is less deformed and the peaked temperature region inside the island is narrower.

In addition to this temperature information, the Thomson scattering system is also capable of providing the density profiles at a rate of 5 kHz (fast compared to the 1 kHz island rotation). A typical example after excitation of the mode, before application of ECRH, is presented in Figure 7. Here, a clear peaking of n_e inside the island is observed. Since the T_e profile inside the island at this stage is flat, a peaked pressure profile results.

An automatic algorithm is used to extract the main island parameters, its width and amplitude, from the ECE-I data. The time evolution of these parameters is given in Figure 8. Knowing the T_e profile and the power deposited inside the island, the diffusivity χ_e in the island can directly be calculated from simple power balance calculations. It turns out that χ_e is 1-1.5 m^2/s , close to the value found for the ambient plasma, which amounts to 1 m^2/s [14].

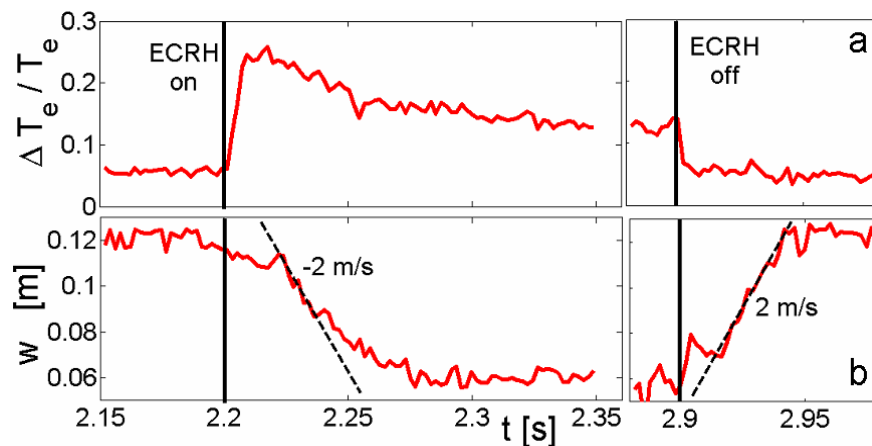


Figure 8: Typical evolutions of the temperature peaking inside the island (a) and the island width w (b) after switching on and off of ECRH, in case of island excitation by the DED.

The evolution of the island width is governed by the modified Rutherford equation. For the special case under consideration here, the island evolution is in addition to the normal stability term of Δ' expanded by a destabilizing term due to the action of the DED (giving rise to shielding currents inside the island to counteract) and a stabilizing term due to the heating effect of the ECRH (the reduced resistivity allows for an enhancement of the induced current inside the island). The mathematical expression for this equation then looks like:

$$0.82\tau_r \frac{dw}{dt} = r_s^2 \Delta' + M_{DED} - M_{ECRH} \quad 2$$

where τ_r is the current diffusion time, w the island width, and r_s the resonant surface. The DED term ($M_{DED} = 2 m r_s (w_{vac}/w)^2$); w_{vac} being the vacuum island width, about 4 cm for this case) is fully known and the ECRH term can be evaluated numerically using the measured T_e data inside the island. Finally the Δ' term can be estimated from the balance in the saturated state. Thus this TEXTOR experiment is unique in the sense that it can separate single terms in the Rutherford equation. The stabilizing effect of heating on the island evolution can thus be calculated, and it is the dominating effect in the island stabilization. Heating may well play a role in NTM stabilization in ITER as well and, consequently, result in lower power requirements for this in ITER [14].

5. Conclusion

Detailed and well controlled investigations into sawtooth and tearing mode physics have been performed on TEXTOR. They confirmed the possibility to control the sawtooth period by changing the shear around the $q=1$ surface in agreement with the critical shear model. The excitation of the $m=2$ tearing modes depends strongly on the rotational difference between the plasma and the perturbation field, and happens as soon as their difference equals the electron diamagnetic frequency. Suppression of $m=2$ tearing modes was obtained as a result of heating inside the island. This effect might relax the constraints on the ECRH power requirements for ITER. High resolution 2D T_e imaging data were crucial for the interpretation and understanding of the physics mechanisms at play.

Acknowledgement

This work, supported by the European Communities under the contract of Association between EURATOM/FOM, was carried out within the framework of the European Fusion Program with the ECEI system developed under US DOE funding. The views and opinions expressed herein do not necessarily reflect those of the European Commission.

References

- ¹ H. K. Park et al., *Rev. Sci. Instrum.* **74** (2004) 4239.
- ² H.J. van der Meiden et al, accepted for publication in *Rev.Sci. Instrum.* 2006.
- ³ E. Westerhof E et al, *Nucl. Fusion* **43** (2003) 1371
- ⁴ K.H. Finken K H (Ed.), *Special Issue: Dynamic Ergodic Divertor Fusion Eng. Design* **37** (1997) 335
- ⁵ H.K. Park et al., *Phys. Rev. Lett.* **96** (2006) 195003
- ⁶ H.K.Park et al, *Phys. Plasmas* **13** (2006) 055907
- ⁷ H.K. Park et al., **Phys. Rev. Lett.** **96** (2006) 195004
- ⁸ F.Porcelli, D. Boucher, M.N. Rosenbluth, *Plasma Phys. Control. Fusion* **38** (1996) 2163
- ⁹ A. Merkulov et al., in: “*Theory of Fusion Plasmas*”, Proc. Of Int. Workshop on Theory of Fusion Plasmas, Varenna, Italy, J.W. Connor, O. Sauter, and E. Sindoni (Editors), Soc. Italiana di Fisica, Bologna (2004) 279.
- ¹⁰ H.R. Koslowski et al, *Nucl. Fusion* **46** (2006) L1; H.R. Koslowski et al, subm. to *Plasma Phys. Contr. Fusion*
- ¹¹ Y. Kikuchi et al, *Phys. Rev. Lett.* **97** (2006) 085003
- ¹² K.H. Finken et al. *Phys. Rev. Lett.* **94** (2005) 015003
- ¹³ E. Westerhof et al., submitted to *Nuclear Fusion* (2006)
- ¹⁴ I.G.J. Classen et al., submitted to *Phys./Rev. Lett.* (2006)